POLITECNICO DI TORINO
Repository ISTITUZIONALE

Independence on the lead of the identification of the ventricular depolarization in the electrocardiogram in wearable devices

Original
Independence on the lead of the identification of the ventricular depolarization in the electrocardiogram in wearable devices / Giordano, N., Cannone, S., Balestra, G., Knaflitz, M.. - In: COMPUTER METHODS AND PROGRAMS IN BIOMEDICINE UPDATE. - ISSN 2666-9900. - ELETTRONICO. - 8:(2025). [10.1016/j.cmpbup.2025.100196]

Availability:
This version is available at: 11583/3000858 since: 2025-06-11T14:33:35Z

Publisher:
Elservier

Published
DOI:10.1016/j.cmpbup.2025.100196

Terms of use:

This article is made available under terms and conditions as specified in the corresponding bibliographic description in the repository

Publisher copyright

(Article begins on next page)

19 November 2026

Computer Methods and Programs in Biomedicine Update 8 (2025) 100196

Contents lists available at ScienceDirect

Computer Methods and Programs in Biomedicine Update

journal homepage: www.sciencedirect.com/journal/computer-methods-and-programs-in-biomedicine-update

Independence on the lead of the identification of the ventricular depolarization in the electrocardiogram in wearable devices

Noemi Giordano *, Silvia Cannone, Gabriella Balestra, Marco Knaflitz

Department of Electronics and Telecommunication and PoliToBIOMed Lab, Politecnico di Torino, Italy

ARTICLE INFO

Keywords:
Wearable devices
Home monitoring
Cardiac time intervals
Electrocardiography
R-wave marker

ABSTRACT

Goal: The home monitoring of cardiac time intervals reduces hospitalization and mortality of cardiovascular patients. However, a reliable time reference in the electrocardiogram is necessary. Nevertheless, the use of different single leads, typical of wearable devices, impacts the repeatability of the time reference and thus the accuracy of the time-dependent parameters. This work proposes a simple approach to detect the peak and onset of the ventricular depolarization, and demonstrates its lead independence, which makes it suitable for wearable devices even with non-standard leads.

Methods: Our method grounds on an energy-based approach, which we applied on a) a publicly available dataset with standard 12-lead recordings; b) a proof-of-concept dataset including a custom precordial non-standard lead implemented on a wearable device.

Results: Compared against the Pan-Tompkins algorithm, our method reduced the absolute error between each lead and the first standard lead by 26 % to 64 % for the peak, and by 70 % to 82 % for the onset detection. The achieved consistency across leads is compatible with clinical monitoring. The computational time was also reduced by 65 % to 96 %, making the algorithm suitable for use on microcontroller-based wearable devices.

Conclusions: The proposed method enables the identification of a stable reference of the ventricular depolarization regardless of the choice of the lead. The presented results open to the implementation on wearable devices for chronic disease monitoring purposes.

Introduction

The latest decades have witnessed a growth in the design, development, and use of wearable technologies in healthcare [1–3]. The application of wearables for telemonitoring is promising for the long-term management of chronic diseases [4,5]. The management of chronic patients at their domicile increases both the quality of care and the quality of life for the patients, while reducing the costs and burden for the healthcare systems [5,6]. Many chronic conditions consist of a long stable phase interrupted by acute episodes. These have the highest impact on both hospital admissions and mortality [7].

Wearables provide a solution for personalized monitoring the health status of chronic patients and prevent acute episodes: when integrated into a telemedicine framework, data from wearables can be used to trigger alarms when the patient's condition deteriorates and timely prevent the acute episode. In this sense, they contribute data to systems that will implement AccuMedicine, recently identified as one of the themes at the interface between engineering and medicine [8].

The monitoring of some cardiovascular chronic conditions relies on time-related biomarkers, which can be referred to as Cardiac Time Intervals (CTI). Examples are the duration of the QRS complex or the QT interval, extracted from the ECG alone, and the electromechanical activation time or the left ventricular systolic time, when the ECG is accompanied by a mechanical signal. When monitoring CTIs, the onset or the peak of the ventricular depolarization extracted from the electrocardiogram (ECG) are typically used as references. These have been associated with respectively the Q-wave and the R-wave. Nevertheless, Q- and R-waves have an intrinsic morphological definition but the morphology of the ECG strongly depends on the lead [9–11]. Fig. 1 shows the morphology of the same heartbeats over the 12 standard leads.

The definition of the Q- and R-waves typically refers to the first standard lead (lead-I), which requires the application of the electrodes on the limbs [11]. This is often unfeasible in wearables: the design of a wearable device must consider many aspects related to the usability, portability, and comfort of use, which depend on the location of the

* Corresponding author at: Politecnico di Torino, Corso Duca degli Abruzzi 24 10129, Torino, Italy.
E-mail address: noemi.giordano@polito.it (N. Giordano).

https://doi.org/10.1016/j.cmpbup.2025.100196

Available online 2 June 2025
2666-9900/© 2025 Published by Elsevier B.V. This is an open access article under the CC BY-NC-ND license (http://creativecommons.org/licenses/by-nc-nd/4.0/).

electrodes [12]. For this reason, when designing a wearable device, the use of non-standard leads is common [13].

The detection of Q- and R-wave peaks, as performed by the Pan-Tompkins algorithm [14], results in estimate errors on different leads. Since these errors are repeatable, they do not invalidate the estimate of the heart rate. However, they could negatively affect the estimate of CTIs [13,15]. Grounding the time reference for CTIs estimation on Q- or R-waves may result in estimate errors, when non-standard leads are employed.

This work shows how to identify the fiducial points corresponding to the ventricular depolarization in the ECG using a non-standard lead. Our goal is considering a simple method for the identification of the onset and peak of the ventricular depolarization and demonstrating its independence on the lead. To achieve our goal, we compare the independence of the results obtained using our method against Pan-Tompkins algorithm applied to a publicly available 12-lead dataset and a proof-of-concept dataset with simultaneous recordings of lead-I and a precordial non-standard lead.

Materials and methods

Public dataset including standard 12-leads recordings

We tested our method on a public dataset of standard 12-lead recordings created by Zheng et al. in 2022 and available on PhysioNet [16]. The dataset includes 45,552 patients: 18 % present a sinus rhythm, the remaining present arrhythmias including sinus bradycardia, atrial fibrillation, sinus tachycardia, atrial flutter, sinus irregularity, supraventricular tachycardia, atrial tachycardia, atrioventricular node reentrant tachycardia, atrioventricular reentrant tachycardia, and wandering atrial pacemaker [17]. Signals were converted with a 32-bit resolution and with a sampling frequency of 500 Hz. A 10 s recording was performed on each patient at rest and included in the dataset, for a total of 589,848 heartbeats.

Custom wearable-based dataset including standard and non-standard leads

After assessing our approach on the 12-lead dataset, we tested its generalizability to non-standard leads. The identified non-standard lead followed the positioning of the electrodes in a real wearable device designed to monitor the CTIs from ECG and heart sounds [18]. Therefore, it provides a real-life application scenario.

In our experimental protocol, we enrolled 39 subjects with no history of cardiovascular diseases. Subjects were asked to lay supine on an examination table with a bare chest. We performed the ECG recordings using a commercial 4-channel system for the recording of biomedical signals (ReMotus™ by ItMed, Torino, Italy). Signals were converted with a 24-bit resolution and with a sampling frequency of 1 kHz.

Two channels were used to simultaneously acquire two ECG leads. The first channel acquired lead-I, the second channel acquired the non-standard lead. We placed the first recording electrode over the second left intercostal space, 5 cm from the sternal border, and the second one 11 cm below. The first channel acquired a lead-I ECG. Fig. 2 presents the location of the electrodes. For each subject, we performed a 5-minute recording: a total number of 13,132 heartbeats was included in the dataset. The experimental protocol was approved by the Ethical Committee of Politecnico di Torino (protocol number 27,801/2023).

Pre-processing

For each recording of the two datasets, each lead was analyzed separately. First, digital filtering was performed to reduce the effect of noise and interferences. The baseline wandering was removed by means of a moving median filter with a window duration of 100 ms. The resulting signal was then filtered with a FIR low-pass filter (250

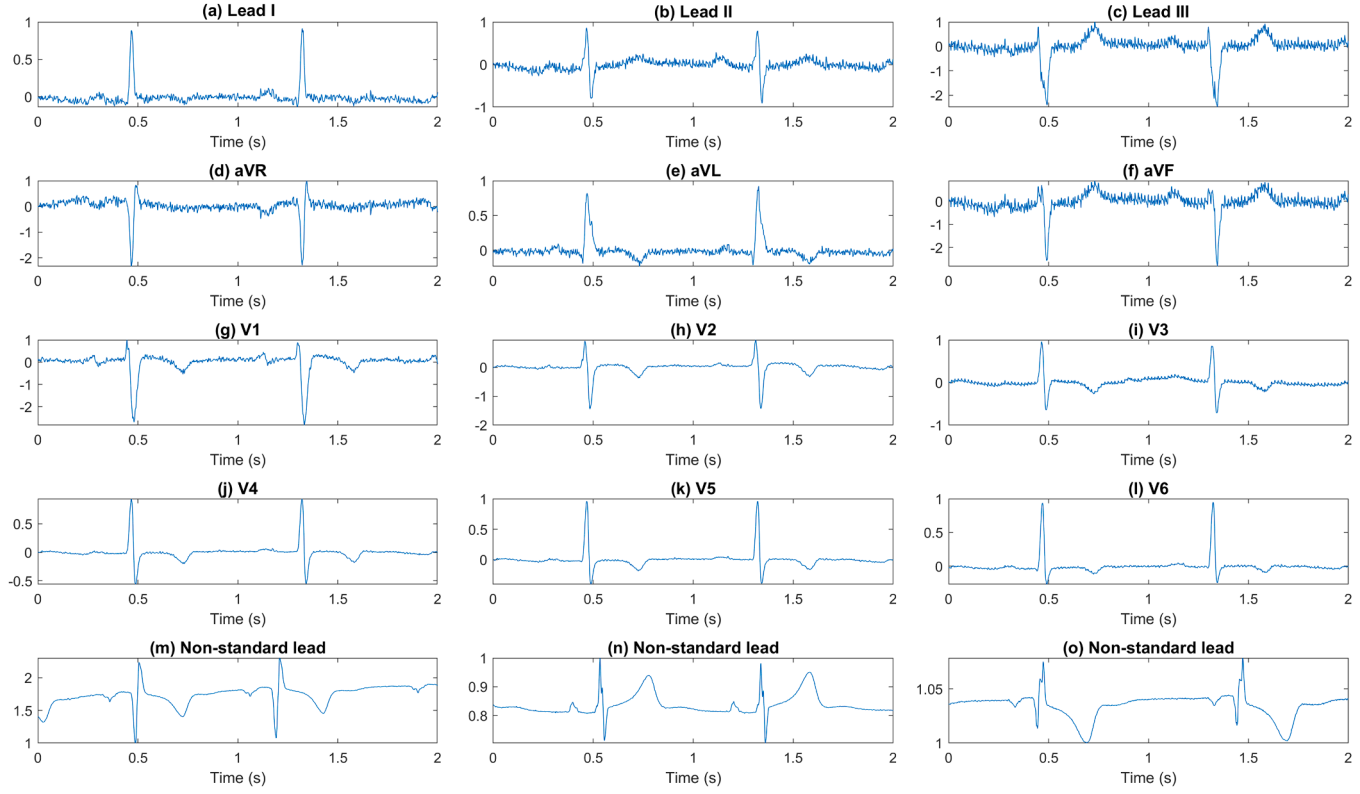


Fig. 1. Sample 5 s ECG segment from the same subject over the 12 standard leads (panels a to l). Sample of 5 s ECG from three different subjects using the same non-standard lead (panels m to o).

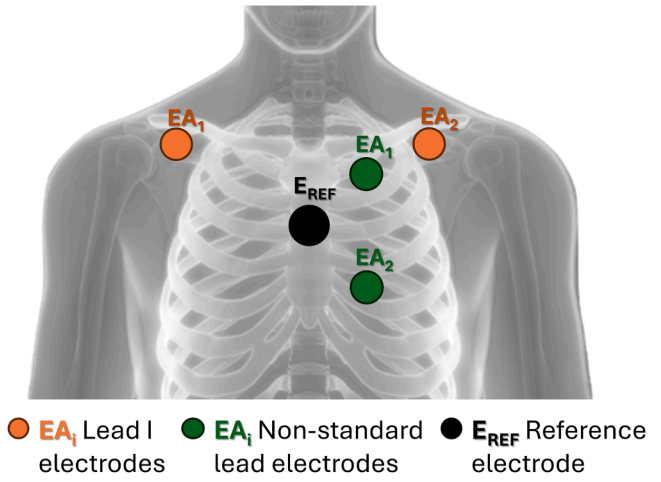


Fig. 2. Positioning of the electrodes in our experimental protocol, aimed at replicating a lead-I and creating a custom non-standard lead.

coefficients) with a cut-off frequency at 40 Hz, which is the limit of the frequency content of the QRS-complex. Realignment of the ECG was required to compensate for the FIR delay.

Traditional identification of the Q- and R-waves

Traditionally, the Q-wave peak is used as reference for the onset of ventricular depolarization, whereas the R-wave peak is used as reference for its maximum. The identification of the standard fiducial points was carried out using the Pan-Tompkins algorithm [14]. This algorithm demonstrated an accuracy of 99.3 % [14]. Even if a wide number of more recent algorithms for the detection of ECG fiducial points exist, Pan-Tompkins is still considered a gold standard in the field. Moreover, the goal of this work is not to increase the detection accuracy (achieved by many previous works), but to study the lead-independence of the method. Therefore, given its undeniably high accuracy in detecting the Q- and R-wave peaks using the ECG morphological characteristics, Pan-Tompkins can be used as a reference for the morphological-based detection in this work, as opposed to the proposed energy-based detection. Fig. 3 shows the amplitude and energy of a sample heartbeat with the detected Q- and R-waves.

Proposed identification of the peak and onset of the depolarization

In our approach, we detected the ventricular depolarization fiducial points on the signal Shannon Energy Envelope (SEE). SEE-based algorithms showed excellent detection performances even in noisy recordings, at a low computational cost [19]. The SEE of a signal x is defined as:

$$SEE = real\left(-x^2 * \log(x^2)\right) \quad (1)$$

The envelope was smoothed using a 50 ms median filter. The filter window length was optimized to generate clear single peaks considering the typical duration of the QRS complex (80 to 120 milliseconds). Moreover, the SEE values below the median were set to zero, to decrease the probability of noise-related artifacts.

Peak of the depolarization

The peak of depolarization was obtained as the peak of the SEE of each heartbeat. The peak identification was performed using a three-step double thresholding approach. In each step, amplitude and time thresholds were defined. All thresholds were defined in function of the maximum SEE value (amplitude thresholds) or in function of the sampling frequency (time thresholds), to make the algorithm adaptive to the peculiarity of the subject's cardiac cycle.

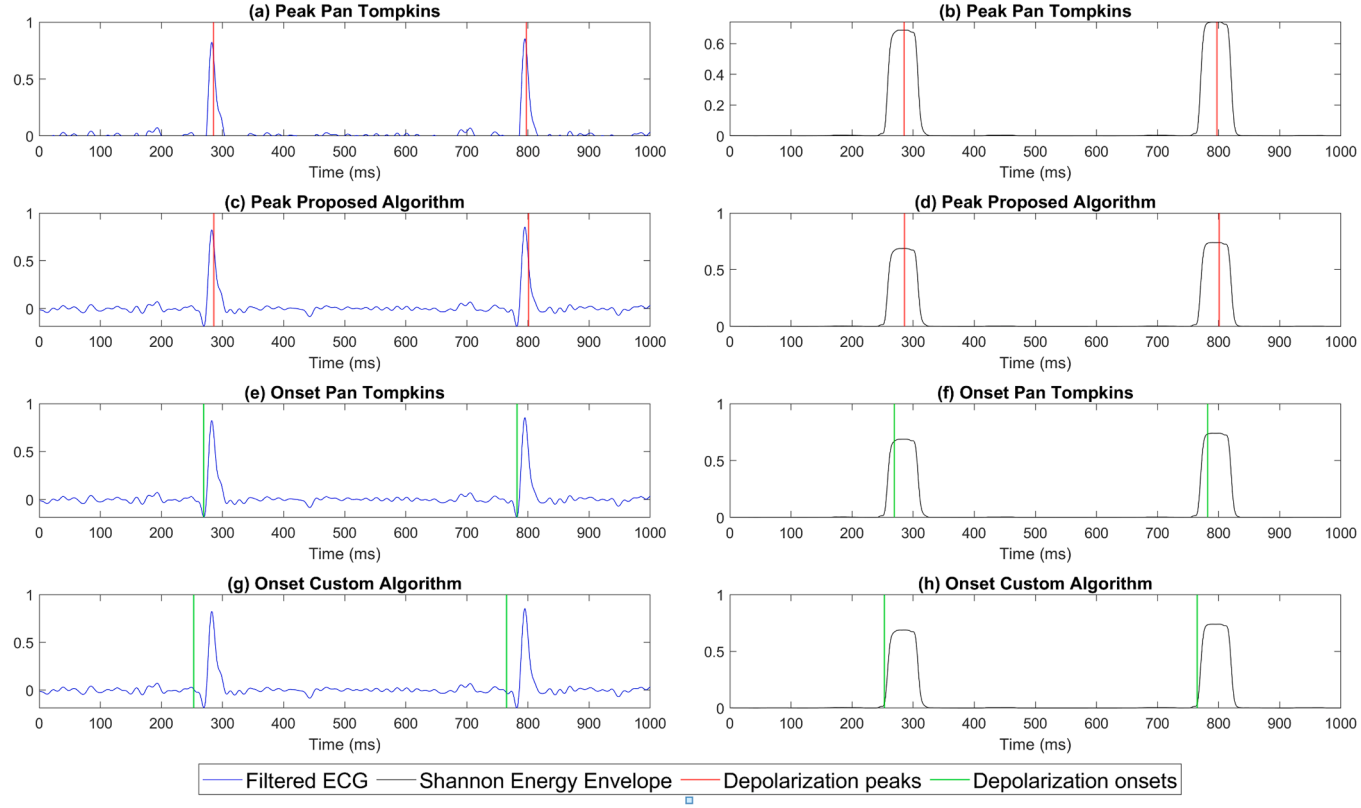


Fig. 3. Example of R peak detection and onset detection with Pan Tompkins and the custom algorithm, respectively (a) to (d) for depolarization peaks detection, (e) to (h) for depolarizionot onset detection.

In the first step, the amplitude threshold value was set to 30 % of the maximum SEE value and the time threshold was set to 20 % of the sampling interval. The amplitude threshold was used as the minimum height for a peak to be considered as a potential QRS complex; the time threshold as the minimum distance between consecutive peaks. The second step is performed if a heart rate lower than 40 bpm is detected. In this case, the amplitude threshold is reduced by 50 % of the 99th percentile. The rationale is that the maximum value may be impacted by the presence of artifacts, whereas the 99th percentile is more robust. RR intervals are scored as differences between identified subsequent peak instants. The third step is performed only in heartbeats showing an RR interval longer than four times the average RR interval. In this case, a further iterative peak search was carried out, whereby the amplitude threshold value was reduced to 80 % at each new iteration. The search for undetected peaks was terminated at the third iteration or when no new peaks were found. No time threshold is used in this phase, but, at the end, false positives, i.e., peaks within an interval equal to the 20 % from another peak with a higher SEE value, were removed.

Onset of the depolarization

SEE presents positive values in correspondence of the QRS-complex segments, and zero values elsewhere. For each heartbeat, the onset of the depolarization was defined as the beginning of the SEE positive segment.

To find the onset of the depolarization segment, a tangent-based approach was designed to detect the most significant rise in the energy contribution. Initially, a search interval was defined by setting an amplitude threshold to 30 % of the maximum SEE value and considering one hundred samples beforehand. The intersection between the tangent of the SEE at the first point of the search interval and the maximum-tangent point was used as reference. The Euclidean distance between each point of the search interval and the tangent intersection was computed and the index of the SEE sample with the minimum Euclidean distance from the tangent intersection. The designed tangent-based approach enables a robust threshold-independent identification of the onset regardless of the morphology of the QRS-complex energy peak.

Fig. 3 shows an example of the detected onset points in the time and energy domains on a sample heartbeat.

Analysis of the results

The analysis answered three research questions:

1. Are the identified points sensitive to the choice of the lead?
2. Does the lead consistency depend on the quality of the recording?
3. Does our method reduce the computational cost of the identification?

The lead-independence was assessed by estimating the error of identification of the fiducial points against the same points identified on lead-I. In case the number of detected fiducial points was not equal on all leads, the fiducial points belonging to the same heartbeat were matched by minimizing the Euclidean distance. The lead-specific error was determined as the Root Mean Square Error (RMSE) among the reference points of lead-I and those of the lead under analysis. The recording-specific error was determined as the average value of the lead-specific errors.

The quality of each signal was assessed to determine whether the identification error depends on the signal quality. We used the Signal-to-Noise Ratio (SNR) as quality metrics, defined as the ratio between the peak-to-peak amplitude of the QRS-complex and four times the standard deviation of noise, estimated between the 70 % and the 85 % of each heartbeat, when no electrical event should occur. The SNR was computed beat-by-beat and averaged over each recording. Afterwards, the correlation between the lead-specific error and the corresponding SNR was computed.

The average computational time of the two methods was measured to estimate their computational cost, with the algorithms running on a notebook computer, Huawei MateBook D, with an 8th Gen Intel(R) Core (TM) i3–8130 U CPU and integrated Intel UHD Graphics 620 GPU.

Results

Comparison Pan-Tompkins vs envelope

Table 1 reports the results of the comparison in terms of average RMSE between each lead and lead-I.

Our algorithm outperforms Pan-Tompkins in both datasets and for both the peak and the onset identification tasks. The significance is even higher on the onset, where our approach reduces the error by 82 % on PhysioNet dataset and by 70 % on our dataset. All reductions proved statistically significant on paired Student *t*-test ($\alpha = 0.05$).

The application on the two datasets shows slightly better results on our dataset than on the publicly available one. This may be due to a lead-dependent difference. To verify this point, we computed the average RMSE separately on each lead. Fig. 4 shows the results.

The RMSE obtained using Pan-Tompkins varies significantly depending on the lead. This is due to the fact that Pan-Tompkins relies on the morphology of the signal: if the lead morphology is similar to lead-I (as in the case of lead-V4) then the RMSE is small, and the other way round. The results obtained using our approach do not depend on the type of lead, since the algorithm relies on the morphology of the signal in the energy domain, which is more consistent throughout the leads. Therefore, the reduction of the RMSE yielded using an energy-based approach is marginal for leads similar to lead-I and more relevant in leads where the signal morphology is highly different from lead-I. Moreover, the RMSE is on average lower using our approach.

Dependence on the signal quality

First, the SNR of all signals was computed for both datasets to investigate if the datasets have consistent quality. The average SNR was found as high as 29 dB (stdev: 5.5 dB) for the 12-lead dataset and 37 dB (stdev: 6.1 dB) for our dataset. The difference proved to be statistically significant at unpaired Student *t*-test (p-value < 0.001).

Fig. 5 shows the RMSE value in function of the SNR of the recording. The error depends on the signal quality, but the dependency is higher for Pan-Tompkins algorithm than for our approach. In the case of our proposed approach, the error can be considered as clinically acceptable (lower than 10 ms) even for reasonably low SNR values (between 5 dB and 10 dB).

Computational time

Table 2 shows an evaluation of the computational time of the two algorithms for recordings lasting 1 min. The interesting aspect is that our approach reduces the computational time by 44 % in case of the peak of the depolarization, and by 96 % for the onset.

Key findings

The results presented in Section III show that the use of Q- and R-waves detected using their amplitude is affected by the choice of the lead. This is valid for both standard and non-standard leads and is in line with the knowledge that the morphology of the QRS complex varies according to the positions of the electrodes. The energy-based envelope is less affected by the lead-specific morphology. This approach significantly reduces the detection error when other leads are compared to lead-I (by 26 % to 82 % depending on the dataset and the fiducial point). The resulting average error is equal to 6 ms for the peak and 3 ms for the onset of the depolarization, which is clinically acceptable. Consistent results were obtained independently on the choice of a standard or non-standard lead, on the presence of arrhythmias, and on the signal quality.

Table 1
Root-mean-square Error.

Point	Dataset	Method	RMSE (ms)	t test p-value
Peak	PhysioNet	Pan Tompkins	8.42 ± 3.84	< 0.001
		Proposed Algorithm	6.29 ± 3.15	
	Recorded	Pan Tompkins	5.96 ± 5.35	0.01
		Proposed Algorithm	2.15 ± 2.06	
Onset	PhysioNet	Pan Tompkins	17.11 ± 6.61	< 0.001
		Proposed Algorithm	3.09 ± 2.64	
	Recorded	Pan Tompkins	11.64 ± 7.65	< 0.001
		Proposed Algorithm	3.51 ± 3.11	

Reported values are averaged over all the leads.

Reported values are averaged over all the leads.

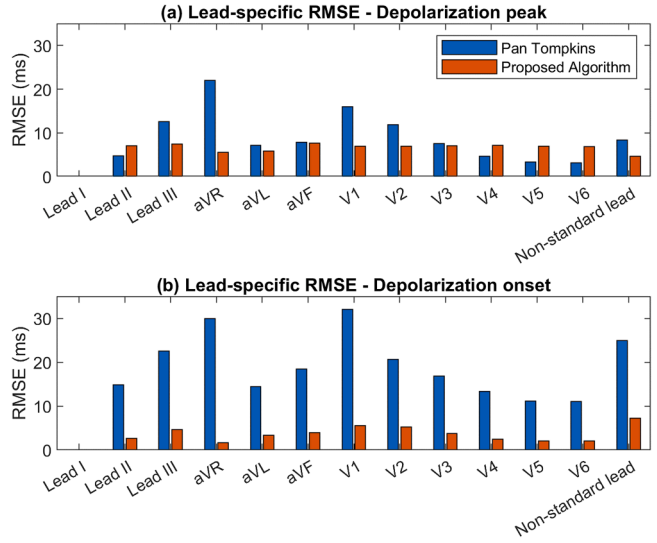


Fig. 4. Lead-specific RMSE, (a) for peaks detection and (b) for onset detection using Pan Tompkins (blue) and our proposed algorithm (red).

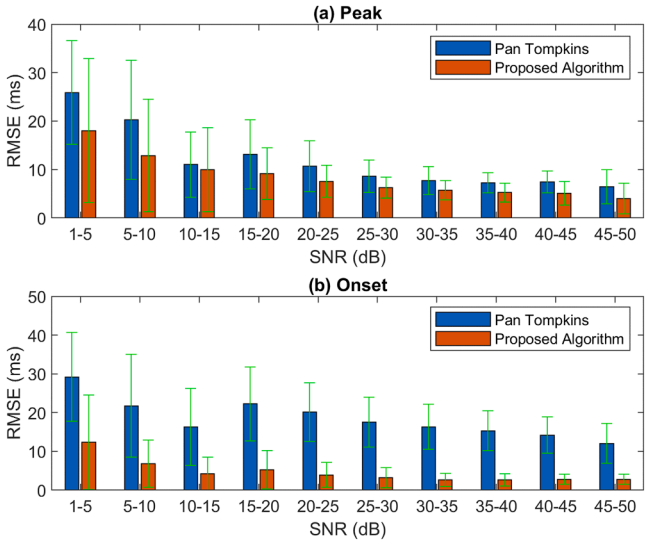


Fig. 5. Dependance of the RMSE on the signal quality, for the detection of (a) peaks, and (b) onsets. Green bars represent the standard deviation.

Moreover, the proposed approach significantly reduced computational time, even when compared to an already low-cost algorithm such as Pan-Tompkins'. The decrease of the identification error as well as the decrease of the computational time are particularly evident on the detection of the onset of the depolarization. This is traditionally considered a more complex task, but the onset is often more relevant from a clinical perspective. This further enhances the potential of our approach.

Discussion

Applicability to wearable devices

The detection of the depolarization fiducial points based on amplitude is highly susceptible to the choice of a different lead. On the contrary, the error obtained using an energy-based approach is more constant, regardless of the choice of the lead. We highlight that multiple algorithms based on energy-based approaches exist in the literature [20, 21] and may produce equally lead-independent performances.

The real advantage of having a lead-independent detector of ventricular depolarization is the possibility of using non-standard leads. Most existing devices for ECG recording in a non-clinical environment ground on the recreation of a lead-I (i.e., KardiaMobile™ by AliveCor and Apple Watch™ by Apple [22]). This limits the integration with other modalities that sometimes require the device to be located on the subject's chest (such as heart sounds recording). In these scenarios, the possibility of designing custom non-standard leads with high accuracy in the identification of the ventricular depolarization opens to novel design possibilities.

We furthermore highlight that the proposed method is applicable to single heartbeats. This enables the use on potentially real-time recording scenarios, and ensures stability even in long-term recordings which may be required in monitoring settings under certain circumstances.

Table 2
Computational time.

Point	Method	Computational time (ms)
Peak	Pan-Tompkins	142.5 ± 14.9
	Proposed Algorithm	78.6 ± 23.6
Onset	Pan-Tompkins	177.8 ± 19.0
	Proposed Algorithm	56.9 ± 11.7

Reported values are averaged over all the leads.

Reported values are averaged over all the leads.

Generalizability of the results

Generalizability is a fundamental requirement for real-life applicability.

The publicly available dataset includes both healthy and pathological subjects, whereas our wearable-based dataset includes healthy subjects only. Given that the same conclusions can be drawn for the two datasets, it can be hypothesized that lead-independence of the proposed approach is not significantly affected by the presence of ECG abnormalities. This will be confirmed by future studies with wearable devices implementing the tested non-standard lead on pathological subjects.

Previous clinical works explored the variability of time parameters (such as the QT interval) over different standard leads [23,24]. To our best knowledge, no previous work investigated the dependence of the detection of the QRS complex on the lead from a technical perspective. Our results on the application of Pan-Tompkins algorithm to different leads (standard and non-standard) confirm the need for such analysis. In fact, an average error of 8 ms was found for the detection of the peak of the depolarization, along with an average error of 17 ms for the detection of the onset of the depolarization. This error can strongly affect the absolute value of the estimate of CTIs. We demonstrated that an energy-based detection technique reduces the error to a clinically acceptable value.

A lead-independent, reliable, time reference of either the peak or the onset of the ventricular depolarization, may open to novel telemonitoring possibilities. For example, it was previously demonstrated that monitoring the QT interval can prevent cardiac arrest due to torsade de pointes triggered by cardioactive drugs [25], but its clinical use is limited by the difficulties in detecting the onset of the QRS-complex and by the choice of the lead, according to clinical guidelines [26]. Our work solves both issues. A similar use case of interest is the monitoring of the duration of the QRS complex, which was proved to predict the occurrence of major adverse cardiac events [27–29]. The utility of a lead-independent time reference is not limited to the use of ECG alone but enables the realization of wearable multimodal devices which integrate ECG electrodes along other kinds of sensors. An example is the monitoring of the CTIs which are index of the electromechanical behavior of the heart and proved effective in predicting adverse events in HF patients [30–33].

Conclusion

This work deals with the identification of lead-independent time references. We employed an energy-based approach and defined the onset and peak of the ventricular depolarization with a simple, low-cost algorithm suitable for use in microcontroller-based devices. The comparison between Pan-Tompkins and our approach involved the use of both a large publicly available dataset including the 12 standard leads in arrhythmic patients and a smaller private dataset including lead-I and a non-standard lead. In both cases, our approach proved effective in reducing the lead-specific error to clinically acceptable values. Our approach also reduced the computational time of the detection by up to 96 %. This reduction is particularly significant when it comes to onset detection, which is traditionally considered a more complex task but has a broader clinical interest. We can conclude that an energy-based approach can open to novel monitoring applications based on time-related biomarkers and wearable devices employing non-standard ECG leads.

CRediT authorship contribution statement

Noemi Giordano: Writing – original draft, Validation, Software, Methodology, Investigation, Formal analysis, Data curation, Conceptualization. **Silvia Cannone:** Writing – original draft, Validation, Software, Methodology, Investigation, Data curation. **Gabriella Balestra:** Writing – review & editing, Supervision, Resources, Project administration. **Marco Knaflitz:** Writing – review & editing, Supervision, Resources, Project administration, Methodology, Funding acquisition, Formal analysis, Conceptualization.

Declaration of competing interest

The authors declare the following financial interests/personal relationships which may be considered as potential competing interests:

Marco Knaflitz reports financial support was provided by Compagnia di Sanpaolo and Links Foundation through a Proof-of-Concept grant (Project CARDIO, PoC Instrument 2020, first cutoff). If there are other authors, they declare that they have no known competing financial interests or personal relationships that could have appeared to influence the work reported in this paper.

Acknowledgements

This work was partially supported by Compagnia di Sanpaolo and Links Foundation through a Proof-of-Concept grant (Project CARDIO, PoC Instrument 2020, first cutoff).

References

[1] A. Azizan, W. Ahmed, A.H.A. Razak, Sensing health: a bibliometric analysis of wearable sensors in healthcare, Health Technol. (Berl). 14 (2024) 15–34, https://doi.org/10.1007/s12553-023-00801-y.

[2] A. Hughes, M.M.H. Shandhi, H. Master, J. Dunn, E. Brittain, Wearable devices in cardiovascular medicine, Circ. Res. 132 (2023) 652–670, https://doi.org/10.1161/CIRCRESAHA.122.322389.

[3] E. Escobar-Linero, L. Muñoz-Saavedra, F. Luna-Perejón, J.L. Sevillano, M. Domínguez-Morales, Wearable health devices for diagnosis support: evolution

and future tendencies, Sensors 23 (2023) 1678, https://doi.org/10.3390/s23031678.
[4] M.M. Baig, H. GholamHosseini, A.A. Moqeem, F. Mirza, M. Lindén, A systematic review of wearable patient monitoring systems – Current challenges and opportunities for clinical adoption, J. Med. Syst. 41 (2017) 115, https://doi.org/10.1007/s10916-017-0760-1.
[5] G. Pare, M. Jaana, C. Sicotte, Systematic Review of Home Telemonitoring for chronic diseases: the evidence base, J. Am. Med. Informatics Assoc. 14 (2007) 269–277, https://doi.org/10.1197/jamia.M2270.
[6] A. Hashemi, S. Nourbakhsh, P. Tehrani, A. Karimi, Remote telemonitoring of cardiovascular patients: benefits, barriers, new suggestions, Artery Res. 22 (2018) 57–63, https://doi.org/10.1016/j.artres.2018.04.001.
[7] M. Gheorghiade, L. De Luca, G.C. Fonarow, G. Filippatos, M. Metra, G.S. Francis, Pathophysiologic targets in the early phase of acute heart failure syndromes, Am. J. Cardiol. 96 (2005) 11–17, https://doi.org/10.1016/j.amjcard.2005.07.016.
[8] S. Subramaniam, M. Akay, M.A. Anastasio, V. Bailey, D. Boas, P. Bonato, A. Chilkoti, J.R. Cochran, V. Colvin, T.A. Desai, J.S. Duncan, F.H. Epstein, S. Fraley, C. Giachelli, K.J. Grande-Allen, J. Green, X.E. Guo, I.B. Hilton, J.D. Humphrey, C. R. Johnson, G. Karniadakis, M.R. King, R.F. Kirsch, S. Kumar, C.T. Laurencin, S. Li, R.L. Lieber, N. Lovell, P. Mali, S.S. Margulies, D.F. Meaney, B. Ogle, B. Palsson, N. A. Peppas, E.J. Perreault, R. Rabbitt, L.A. Setton, L.D. Shea, S.G. Shroff, K. Shung, A.S. Tolias, M.C.H. Van Der Meulen, S. Varghese, G. Vunjak-Novakovic, J.A. White, R. Winslow, J. Zhang, K. Zhang, C. Zukoski, M.I. Miller, Grand challenges at the interface of engineering and medicine, IEEE Open J. Eng. Med. Biol. 5 (2024) 1–13, https://doi.org/10.1109/OJEMB.2024.3351717.
[9] B.J.A. Schijvenaars, J.A. Kors, G. van Herpen, F. Kornreich, J.H. van Bemmel, Effect of electrode positioning on ECG interpretation by computer, J. Electrocardiol. 30 (1997) 247–256, https://doi.org/10.1016/S0022-0736(97)80010-6.
[10] P. Kligfield, L.S. Gettes, J.J. Bailey, R. Childers, B.J. Deal, E.W. Hancock, G. van Herpen, J.A. Kors, P. Macfarlane, D.M. Mirvis, O. Pahlm, P. Rautaharju, G. S. Wagner, Recommendations for the standardization and interpretation of the electrocardiogram, Circulation 115 (2007) 1306–1324, https://doi.org/10.1161/CIRCULATIONAHA.106.180200.
[11] V. Fuster, R.A. Harrington, J. Narula, Z.J. Eapen, Hurst's the Heart, McGraw-Hill Medical, 2011.
[12] A. Soroudi, N. Hernández, L. Berglin, V. Nierstrasz, Electrode placement in electrocardiography smart garments: a review, J. Electrocardiol. 57 (2019) 27–30, https://doi.org/10.1016/j.jelectrocard.2019.08.015.
[13] M. Metshein, A. Krivošei, A. Abdullayev, P. Annus, O. Märtens, Non-standard electrode placement strategies for ECG signal acquisition, Sensors 22 (2022) 9351, https://doi.org/10.3390/s22239351.
[14] J. Pan, W.J. Tompkins, A real-time QRS detection algorithm, IEEE Trans. Biomed. Eng. BME 32 (1985) 230–236, https://doi.org/10.1109/TBME.1985.325532.
[15] N. Saghir, A. Aggarwal, N. Soneji, V. Valencia, G. Rodgers, T. Kurian, A comparison of manual electrocardiographic interval and waveform analysis in lead 1 of 12-lead ECG and Apple Watch ECG: a validation study, Cardiovasc. Digit. Heal. J. 1 (2020) 30–36, https://doi.org/10.1016/j.cvdhj.2020.07.002.
[16] J. Zheng, H. Guo, H. Chu, A large scale 12-lead electrocardiogram database for arrhythmia study (version 1.0.0), (2022). https://doi.org/10.13026/wgex-er52.
[17] J. Zheng, H. Chu, D. Struppa, J. Zhang, S.M. Yacoub, H. El-Askary, A. Chang, L. Ehwerhemuepha, I. Abudayyeh, A. Barrett, G. Fu, H. Yao, D. Li, H. Guo, C. Rakovski, Optimal multi-stage arrhythmia classification approach, Sci. Rep. 10 (2020) 2898, https://doi.org/10.1038/s41598-020-59821-7.
[18] N. Giordano, S. Rosati, G. Balestra, M. Knaflitz, A wearable multi-sensor array enables the recording of heart sounds in homecare, Sensors 23 (2023), https://doi.org/10.3390/s23136241.
[19] H. Dogan, R.O. Dogan, A comprehensive review of computer-based techniques for R-peaks/QRS complex detection in ECG signal, Arch. Comput. Methods Eng. 30 (2023) 3703–3721, https://doi.org/10.1007/s11831-023-09916-x.
[20] H. Beyramienanlou, N. Lotfivand, Shannon's energy based algorithm in ECG signal processing, Comput. Math. Methods Med. 2017 (2017) 1–16, https://doi.org/10.1155/2017/8081361.
[21] H. Zhu, J. Dong, An R-peak detection method based on peaks of Shannon energy envelope, Biomed. Signal Process. Control 8 (2013) 466–474, https://doi.org/10.1016/j.bspc.2013.01.001.
[22] L.J. Hoek, J.L.P. Brouwer, A.A. Voors, A.H. Maass, Smart devices to measure and monitor QT intervals, Front. Cardiovasc. Med. 10 (2023) 1–12, https://doi.org/10.3389/fcvm.2023.1172666.
[23] P.M. Rautaharju, B. Surawicz, L.S. Gettes, AHA/ACCF/HRS recommendations for the standardization and interpretation of the electrocardiogram, J. Am. Coll. Cardiol. 53 (2009) 982–991, https://doi.org/10.1016/j.jacc.2008.12.014.
[24] G.K. Panicker, V. Salvi, D.R. Karnad, S. Chakraborty, D. Manohar, Y. Lokhandwala, S. Kothari, Drug-induced QT prolongation when QT interval is measured in each of the 12 ECG leads in men and women in a thorough QT study, J. Electrocardiol. 47 (2014) 155–157, https://doi.org/10.1016/j.jelectrocard.2013.11.004.
[25] B.J. Drew, M.J. Ackerman, M. Funk, W.B. Gibler, P. Kligfield, V. Menon, G. J. Philippides, D.M. Roden, W. Zareba, Prevention of torsade de pointes in Hospital settings, Circulation 121 (2010) 1047–1060, https://doi.org/10.1161/CIRCULATIONAHA.109.192704.
[26] P.M. Rautaharju, B. Surawicz, L.S. Gettes, AHA/ACCF/HRS recommendations for the standardization and interpretation of the electrocardiogram, J. Am. Coll. Cardiol. 53 (2009) 982–991, https://doi.org/10.1016/j.jacc.2008.12.014.
[27] H. Alfraidi, C.M. Seifer, B.M. Hiebert, L. Torbiak, S. Zieroth, W.F. McIntyre, Relation of increasing QRS duration over time and cardiovascular events in outpatients with heart failure, Am. J. Cardiol. 124 (2019) 1907–1911, https://doi.org/10.1016/j.amjcard.2019.09.018.
[28] J. Joseph, B.C. Claggett, I.S. Anand, J.L. Fleg, T. Huynh, A.S. Desai, S.D. Solomon, E. O'Meara, S. Mckinlay, B. Pitt, M.A. Pfeffer, E.F. Lewis, QRS duration is a predictor of adverse outcomes in heart failure with preserved ejection fraction, JACC Hear. Fail. 4 (2016) 477–486, https://doi.org/10.1016/j.jchf.2016.02.013.
[29] X. Chen, P.-O. Hansson, E. Thunström, Z. Mandalenakis, K. Caidahl, M. Fu, Incremental changes in QRS duration as predictor for cardiovascular disease: a 21-year follow-up of a randomly selected general population, Sci. Rep. 11 (2021) 13652, https://doi.org/10.1038/s41598-021-93024-y.
[30] S.H. Sung, C.J. Huang, H.M. Cheng, W.M. Huang, W.C. Yu, C.H. Chen, Effect of acoustic cardiography-guided management on 1-year outcomes in patients with acute heart failure, J. Card. Fail. 26 (2020) 142–150, https://doi.org/10.1016/j.cardfail.2019.09.012.
[31] J. Zhang, W.X. Liu, S.Z. Lyu, Predictive value of electromechanical activation time for In-hospital major cardiac adverse events in heart failure patients, Cardiovasc. Ther. 2020 (2020), https://doi.org/10.1155/2020/4532596.
[32] T.F. Chao, S.H. Sung, H.M. Cheng, W.C. Yu, K.L. Wang, C.M. Huang, C.H. Chen, Electromechanical activation time in the prediction of discharge outcomes in patients hospitalized with acute heart failure syndrome, Intern. Med. 49 (2010) 2031–2037, https://doi.org/10.2169/internalmedicine.49.3944.
[33] J. Shitara, T. Kasai, N. Murata, N. Yamakawa, S. Yatsu, A. Murata, H. Matsumoto, T. Kato, S. Suda, Y. Matsue, R. Naito, M. Hiki, H. Daida, Temporal changes of cardiac acoustic biomarkers and cardiac function in acute decompensated heart failure, ESC Hear. Fail. 8 (2021) 4037–4047, https://doi.org/10.1002/ehf2.13492.